Piotr PRUCHNICKI[1]

13. CORRECTION OF ERRORS OCCURRING DURING THE DETECTION OF PULSE ARRIVAL TIME IN ULTRASOUND TOMOGRAPHY

13.1. Introduction

Breast cancer is one of the most common types of cancer in women [5]. Therefore, fast and precise diagnosis of breast cancer is very important. Currently palpation, X-ray mammography, ultrasound imaging (USG) and magnetic resonance imaging (MRI) are used for this purpose. One of the newest methods of visualizing the internal structure of the breast is ultrasound tomography. This method combines the use of harmless ultrasounds with tomographic imaging methods.

Advanced work towards building a prototype of the ultrasonic tomograph to examine the breasts of women is currently underway at few research centers in the world (Poland, USA, and Germany) [1, 2, 3, 7, 9, 13, 17]. One of the devices is an ultrasound tomograph designed and developed by Dramiński S.A. [11, 12, 14, 15].

The ultrasound circular array of the tomograph consists of 1024 miniature piezoceramic transducers distributed evenly on the inner side of the ring. The electronic data acquisition system generates measurement signals powering the transmitting transducers and collects the signals received by the array transducers after passing through the breast tissue. Next, the parameters of the received ultrasonic signals are determined. Based on these parameters, ultrasonic transmission tomographic images are reconstructed.

13.2. Ultrasound tomography

The principle of operation of the ultrasound tomograph for breast diagnostics consists in generating a measuring impulse by one transmitting transducer and its recording by a large

[1] Department of Acoustics, Multimedia and Signal Processing, Faculty of Electronics, Wroclaw University of Technology, Wyb. Wyspiańskiego 27, 50-370 Wrocław, Poland, Dramiński S.A. Owocowa 17, 10-860 Olsztyn, Poland, piotr.pruchnicki@pwr.edu.pl

number of receiving transducers (Fig. 1). In the next step, the signal is emitted by another transmitting transducer and recording again by the receiving transducers. This algorithm is repeated for all transducers in the ring head of the device.

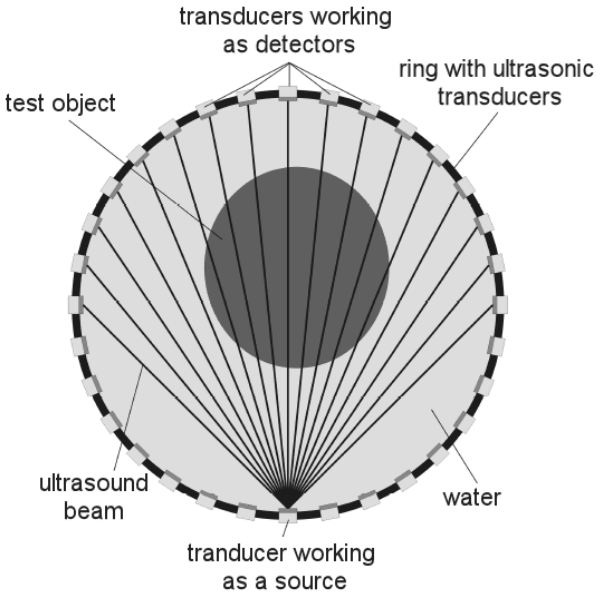

Fig. 1. The principle of operation of an ultrasound tomograph
Rys. 1. Zasada działania tomografu ultradźwiękowego

Acoustic parameters are determined from each signal transmitted through tissue: the average times of arrival of ultrasonic pulses and the average amplitudes of these pulses after passing through the scanned coronal section of the breast [10, 16].

Due to the large amount of data generated during the measurement of a single breast cross-section, their presentation is not easy. The values of the determined parameters are most often presented in the form of a sinogram. A sinogram is a snapshot of the complete measurement data for M rays and N projections. In the case of the described tomograph, the measuring head has 1024 transducers, each of which can work as a signal source. 513 receiver transducers are always active during data recording for the reconstruction of transmission images. This means that we are proceeding with 1024 projections, each consisting of 513 rays.

In the sinogram, the x and y axes correspond to the receiving and transmitting transducers for individual rays, respectively. The sinogram is most often presented as a flat two-dimensional color scale image. Each projection is drawn as a horizontal line, the parameter value measured for a given radius is mapped as a point on the line with a color resulting from the adopted scale. For the purposes of this study, sinograms will be presented in grayscale. Figure 2 shows an example of a sinogram showing the speed of sound and attenuation of the acoustic wave for the same cross-section phantom.

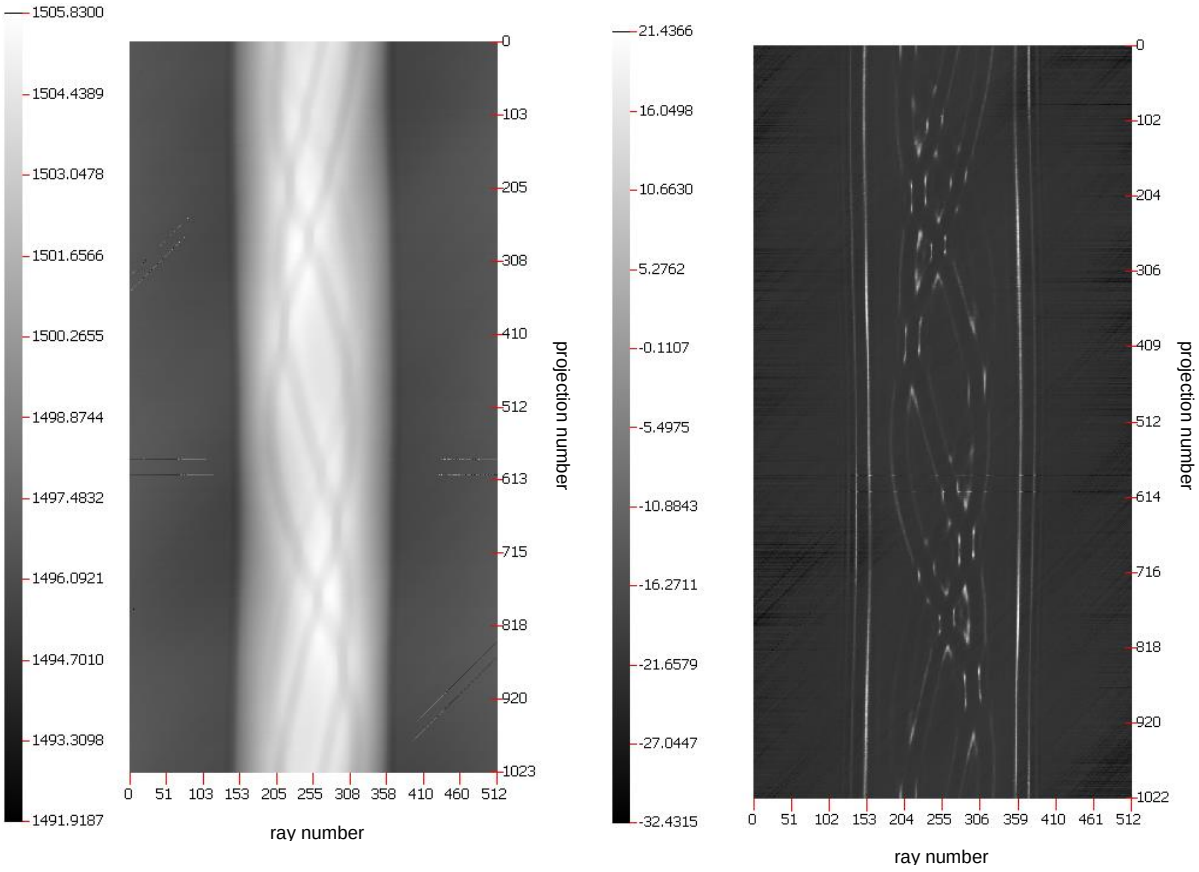

Fig. 2. Sample sinogram showing the speed of sound values (on the left) and values of acoustic wave attenuation (on the right)

Rys. 2. Przykładowy sinogram przedstawiający wartości prędkość dźwięku (po lewej) i wartości tłumienia fali akustycznej (po prawej)

The breast phantom sinograms, as shown in Figure 2, have a regular structure with little changes. The actual breasts are, however, much more complex structures than a simple phantoms. For this reason, the appearance of sinograms is also more complex.

The data presented on the sinograms are the basis for the creation of transmission tomographic images: the distribution of local values of ultrasound speed (speed image) and the distribution of local values of ultrasound attenuation (attenuation image). The transmission images are reconstructed using the filtered back projection algorithm [4, 6, 8]. Fig. 3 shows examples of reconstructed tomographic images of the breast biopsy phantom CIRS Model 059.

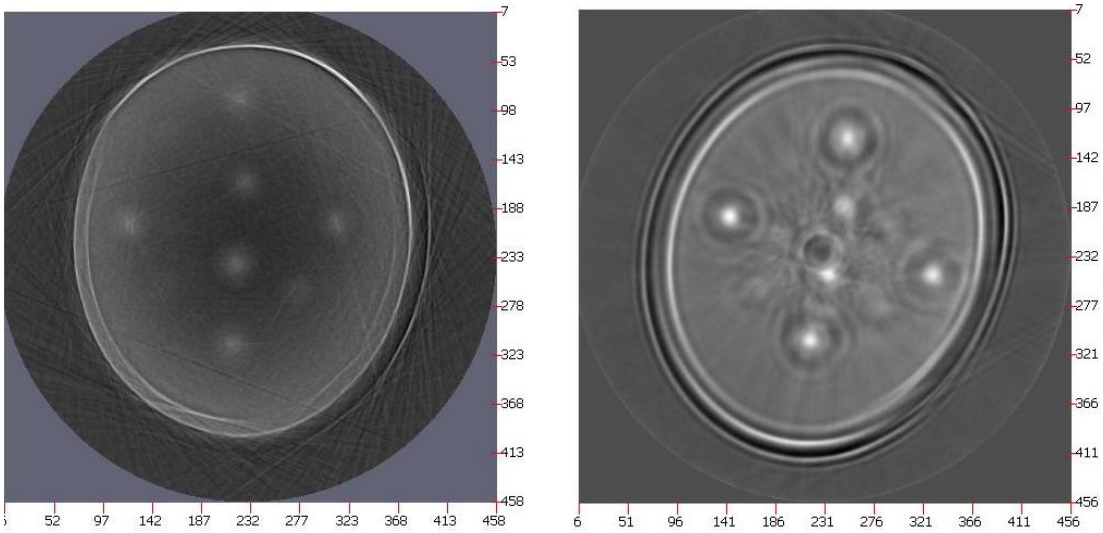

Fig. 3. Sample reconstructed tomographic images of the phantom: speed image (on the left) and attenuation image (on the right)
Rys. 3. Przykładowe zrekonstruowane obrazy tomograficzne fantomu: obraz prędkościowy (po lewej) i obraz tłumieniowy (po prawej)

13.3. Determining the arrival time of the pulse

The pulse arrival time detection algorithm developed for the ultrasound tomograph uses the constant fraction method and zero crossing detection.

The constant fraction method was used to find the half period, which is the first half period of a received pulse. The method of zero crossing detection was used to accurately determine the time of arrival. For this purpose, interpolation was performed between samples with a negative and positive signal value above the noise amplitude for the beginning of the received signal. When digitally measuring the transit time with this method, it is possible to obtain the time resolution much better than the quantization step.

Figure 4 shows examples of recorded measurement pulses after passing through the breast. As can be seen, the shape of the received pulse is not always the same. Case a) presents the impulse closest to the theoretical pattern. Pulses of this shape reach the receiving transducer if the ultrasonic wave passes through a homogeneous structure with low attenuation. These pulses are also recorded when measuring the reference characteristics in the water itself. The remaining examples b) - d) show the shapes of the impulses that occur most frequently after passing through the breast tissue. Their changed shape results mainly from the phenomenon of multipath. The ultrasonic wave passing through the breast is refracted at the boundaries of the structures inside. Thus, the receiving transducer receives phase-shifted, delayed signals that overlap. The distorted shape of the received pulse makes it difficult to develop an algorithm that precisely determines the arrival time.

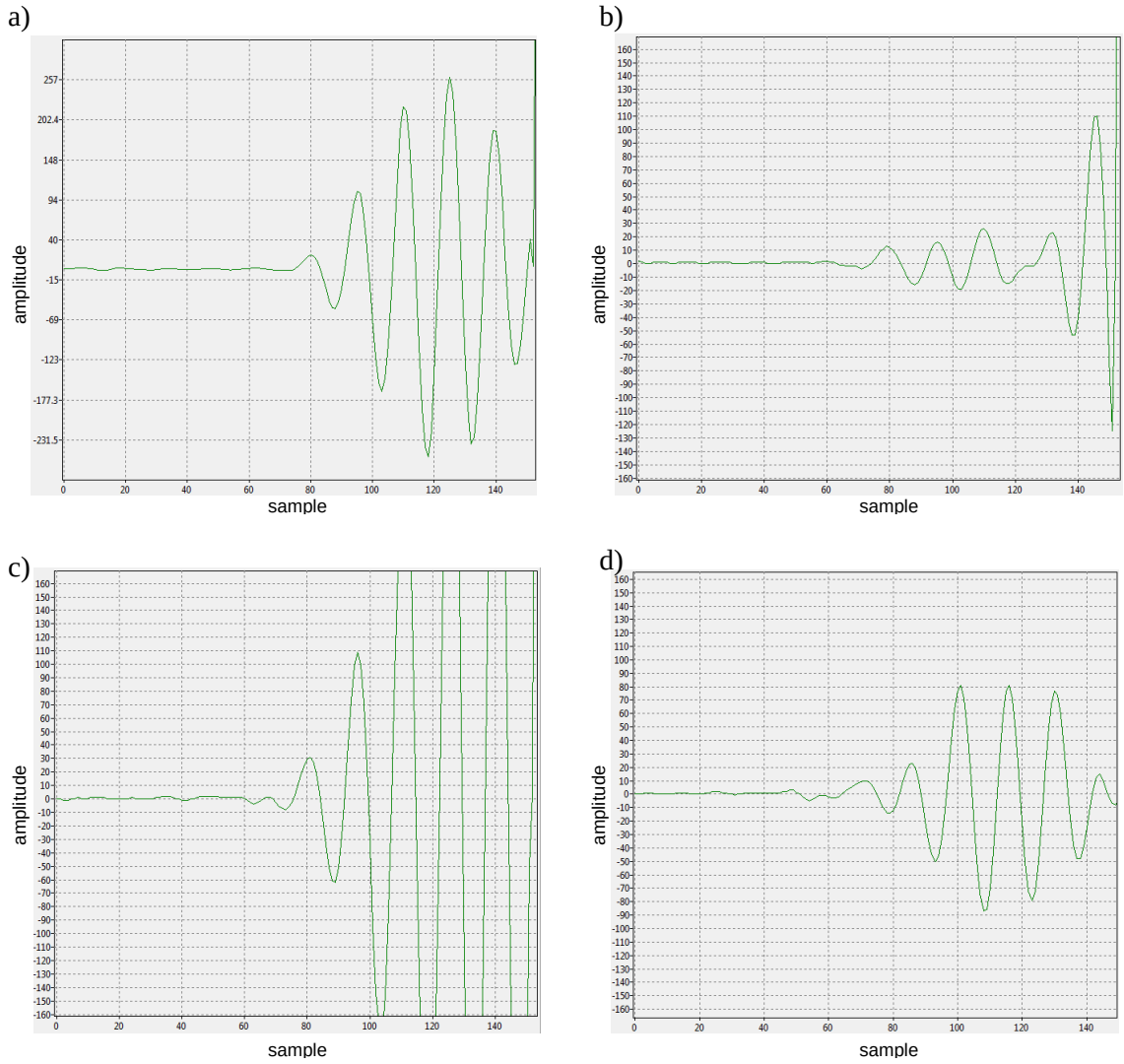

Fig. 4. Sample waveforms of transmission pulses after passing through the breast
Rys. 4. Przykładowe przebiegi czasowe impulsów transmisyjnych po przejściu przez pierś

13.4. Errors occurring during the detection of impulse arrival time

When determining the time of arrival of the impulse, errors appear that negatively affect the reconstructed tomographic images.

The most obvious error is when no signal is recorded. The reasons may be different:

- damage to the ring matrix transducer leads,
- very low efficiency of the transducer, resulting, for example, from damage or assembly errors,
- very high attenuation of the ultrasonic wave on the path between the transmitting and receiving transducer,
- geometry of the examined object (breast), which causes the acoustic wave to refract and not reach the receiver,
- signal dropout caused by the directivity characteristics of the transducers, most often occurring when the angle between the transmitting and receiving transducers is large.

When no signal reaches the receiving transducer, it is not possible to determine the pulse arrival time. Most of these cases (especially those associated with damage to individual transducers) can be identified during the execution of the reference calibration measurement. For these transducers, the arrival time is not determined and its value is determined as the average of the neighboring points of the sinogram.

Due to the uneven shape of the received pulse, errors in its determination sometimes occur during the detection of the arrival time. The most common errors consist in shifting the detection site by a multiple of the periods of the received signal. The mechanism of this type of errors is presented in Fig. 5. Based on the amplitude of the received signal, the detection threshold P1 is determined. Applying this threshold to constant fraction detection leads to setting the pulse start at position A. However, if the received signal has a slightly lower amplitude, the threshold P2 will be set. In this case, a slight change in the threshold will move the detection site to position B.

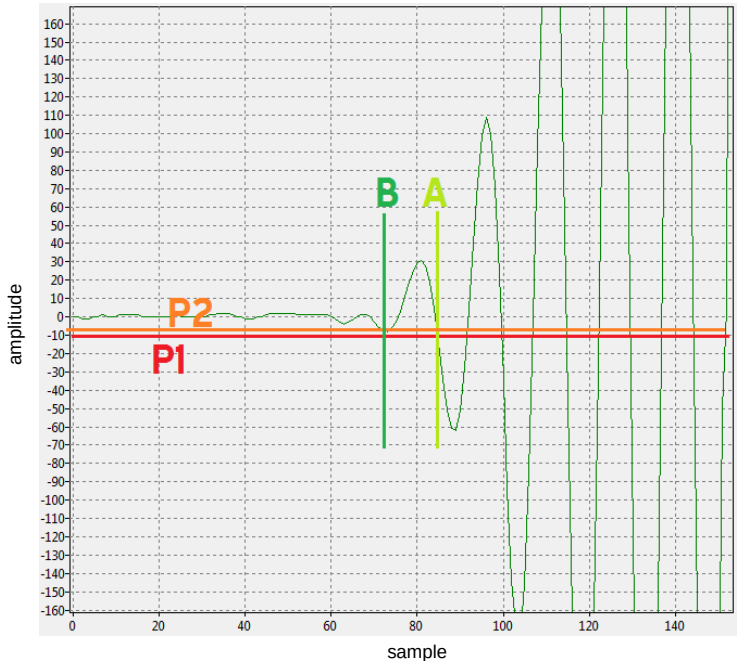

Fig. 5. The occurrence of impulse arrival time detection errors
Rys. 5. Występowanie błędów wykrywania czasu dotarcia impulsu

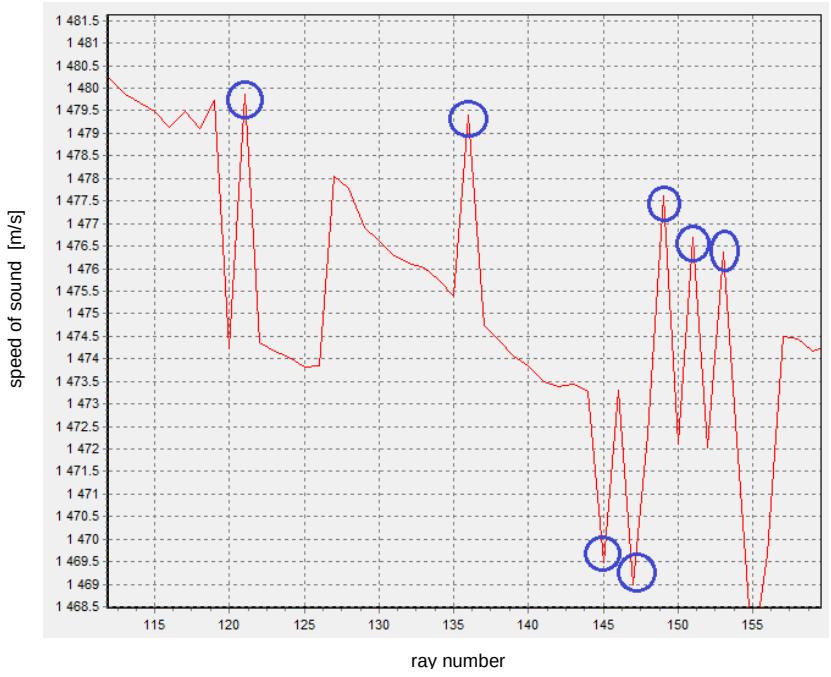

Fig. 6. Examples of errors (marked with circles) resulting from shifting the detection point by one period
Rys. 6. Przykłady błędów (zaznaczone kółkami) wynikających z przeskoku punktu detekcji o jeden okres

The most common errors are single shifts of the detection point by one period. They occur when for a given pair of transducers the detection threshold changes to a small degree in

relation to the neighboring pairs. An example of a sinogram line with such errors is presented in Fig. 6.

The ultrasound ring matrix of the tomograph has diameter D = 260 mm and its elementary transducers operate in the frequency of ca. 2 MHz. Assuming the propagation speed of the ultrasound wave in the breast tissue v = 1540 m/s, the time after which the impulse reaches the opposite transducer of the head is t = 168.83 μs. A shift by one period changes the approach time by Δt = 0.5 μs. The ultrasonic wave propagation speed determined after changing the time differs from the correct one by about 4 m/s. This is clearly seen in Fig. 6.

Apart from errors resulting from shifting the detection point by one period, there are situations when the shift is larger and covers 2, 3 or 4 periods (Fig. 7). Errors related to shifts of more than one period are less frequent and easier to detect. However, their presence in the sinogram causes a greater degradation of the reconstructed result images.

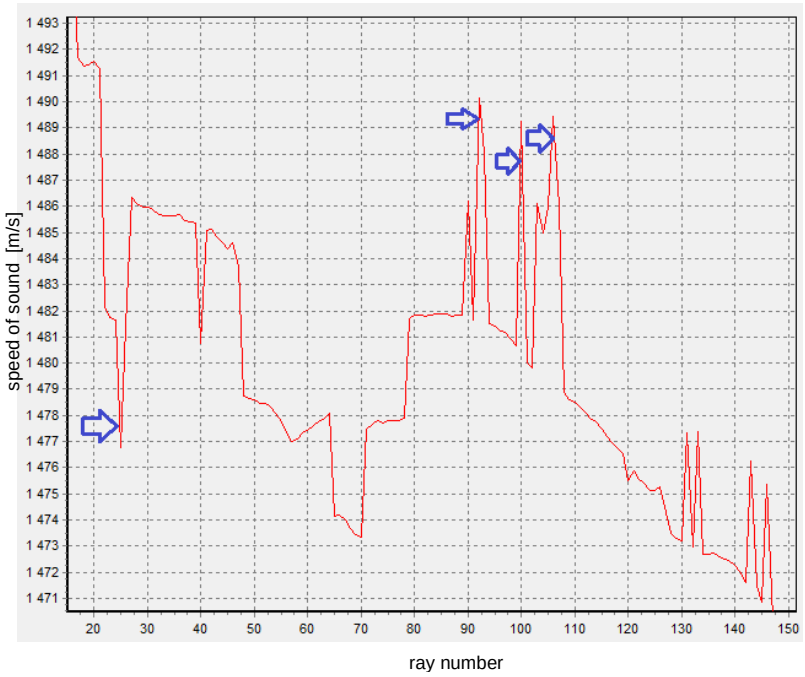

Fig. 7. Examples of errors (marked with arrows) resulting from shifting the detection point by two periods

Rys. 7. Przykłady błędów (zaznaczone strzałkami) wynikających z przesunięcia punktu detekcji o dwa okresy

There are also errors in the determined sinogram, which are manifested by the presence of single speed shifts with a value of several tens m/s. These are usually single points. Errors consisting in a significant reduction in speed result most often from a random fading of the received pulse, which takes the shortest route. The algorithm then detects the impulse that arrived later. A much higher speed most often results from the presence of a disturbance that occurred before the actual impulse. These errors can only be removed by averaging the speed values from the neighboring points of the sinogram.

13.5. Error correction

Figure 8 shows an example of a sinogram obtained during breast measurements with the use of an ultrasound tomograph. The sinogram shows points and lines with speed values significantly different from the average speed value in the breast tissue. The maximum measured speed value exceeds 1700 m/s and the smallest one is below 1190 m/s.

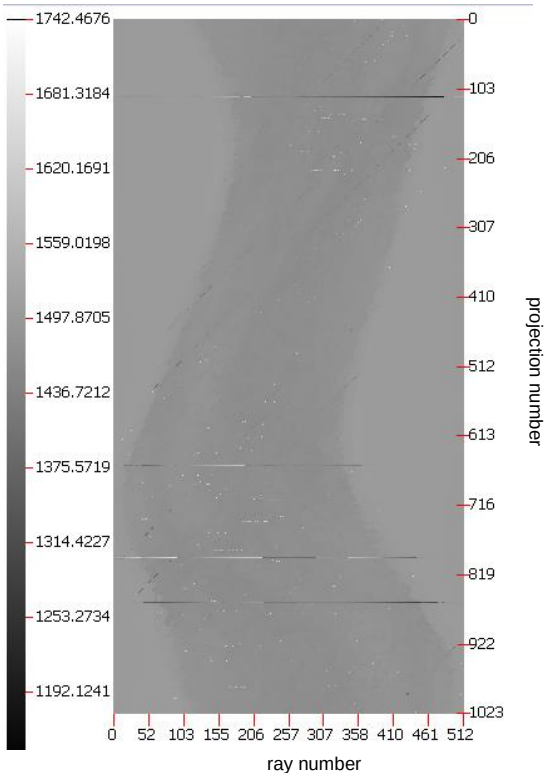

Fig. 8. Sinogram showing the speed of sound values for cross section of the breast without error correction
Rys. 8. Sinogram prezentujący prędkość dźwięku dla przekroju piersi bez korekcji błędów

The reconstruction of breast images from such disturbed sinograms is also charged with significant disturbances. Figure 9 shows the results of breast image reconstruction using two different filter functions. The Hamming filter does not remove fast-changing components from the image, which leads to a highly disturbed reconstruction of the breast cross-section. In contrast, the stochastic filter averages the errors in the image, which improves the legibility of the image at the expense of visibility of details. Both images are additionally characterized by low contrast, which hinders their analysis, the reconstructed speeds are in the range of 1200 - 1600 m/s.

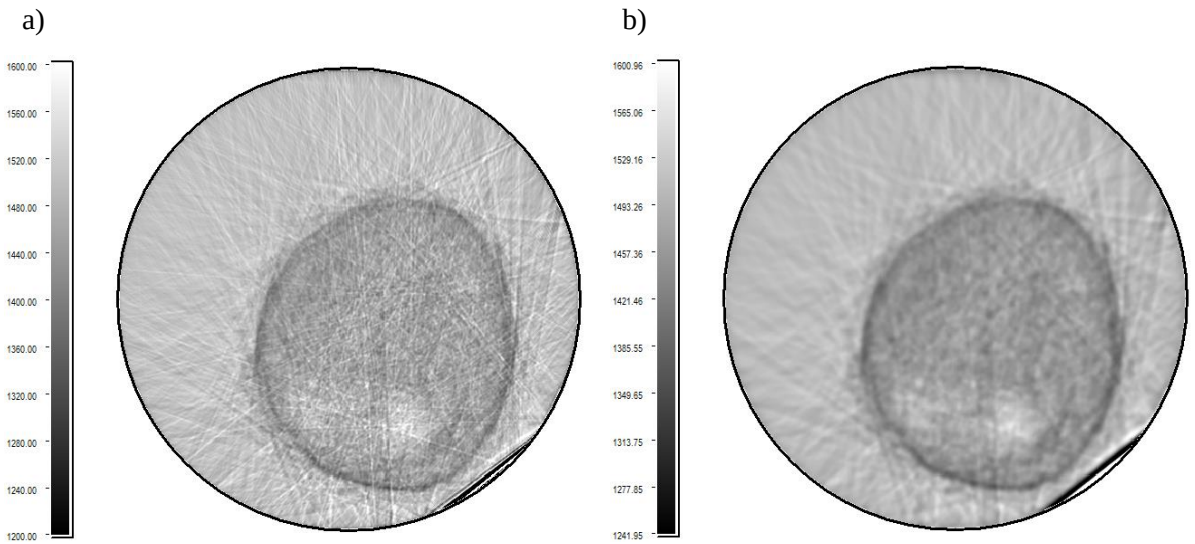

Fig. 9. Reconstructed speed distribution in the cross section of the breast without error correction: with Hamming filter a) with stochastic filter b)
Rys. 9. Zrekonstruowany rozkład prędkości w przekroju piersi bez korekcji błędów: z filtracją Hamminga a) z filtrem stochastycznym b)

13.5.1. Correction of signal dropouts and high value random errors

Due to the very large difference in the speed of the erroneous point in relation to the neighboring points, often over 100 m/s, each such point is reconstructed in the form of a straight line crossing the image (such lines are clearly visible in Figure 9a). A large number of such lines makes it difficult to interpret the results and degrades the quality of the resulting image.

The first step in the correction of a sinogram is therefore the correction of dropouts and large random errors. The only method of obtaining the speed value at such a point is its approximation from the values of the neighboring points of the sinogram.

Figure 10 shows a sinogram corrected in this way. Compared to the sinogram in Fig. 8, the speed range has decreased to 1435 - 1555 m/s. In the example of the sinogram line shown in Fig. 11, we can see the occurrence of only errors consisting in shifting the detection point by 1, 2 or 3 periods.

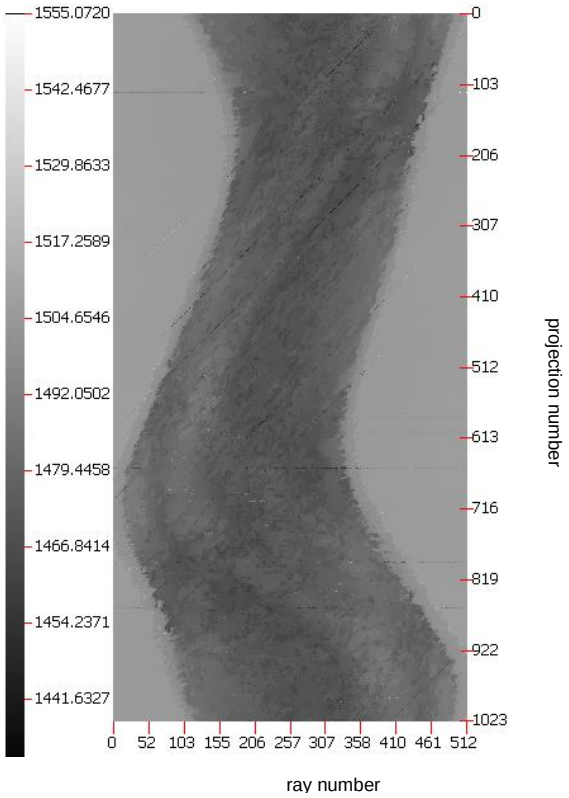

Fig. 10. Sinogram showing the speed of sound values after correction of signal dropouts and large random errors

Rys. 10. Sinogram prezentujący prędkość dźwięku dla przekroju piersi po korekcji zaników sygnału i przypadkowych błędów o dużej wartości

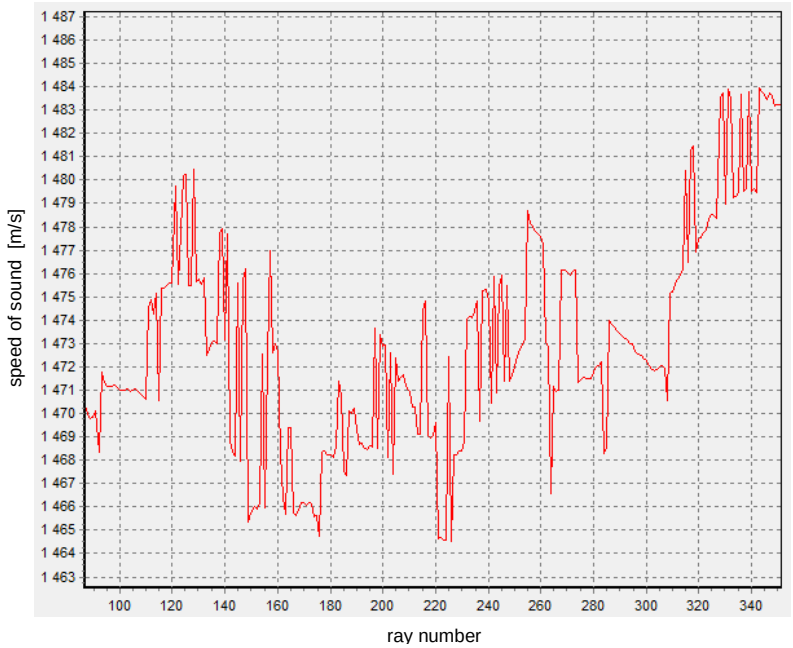

Fig. 11. An example of a sinogram line after correction of signal dropouts and random errors of large amplitude

Rys. 11. Przykład linii sinogramu po skorygowaniu zaników sygnału i błędów losowych o dużej amplitudzie

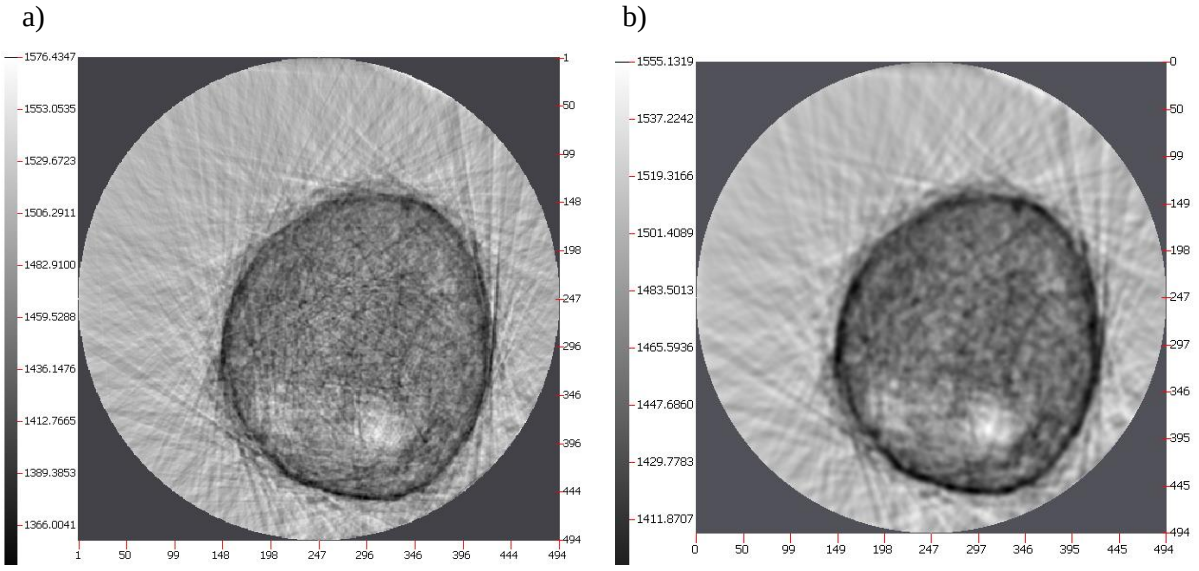

Fig. 12. Reconstructed speed distribution in the cross section of the breast after correction of signal dropouts and random errors of large amplitude: with Hamming filter a) with stochastic filter b)

Rys. 12. Zrekonstruowany rozkład prędkości w przekroju piersi po skorygowaniu zaników sygnału i błędów losowych o dużej amplitudzie: z filtracją Hamminga a) z filtrem stochastycznym b)

In the reconstructed images shown in Fig. 12 (especially when filtered with a Hamming filter) it can be seen that the interfering lines have a much smaller amplitude. The contrast of the image also improved, the reconstructed speeds are in a narrower range of 1410 - 1550 m/s.

13.5.2. Sinograms after correction of single detection point shifts

The distorting lines that appear after reconstruction are caused by points in the sinogram where the detection point has shifted. The next correction step is therefore to remove such single shifts from the sinogram.

The correction algorithm has to look through the sinogram line by line and find for a speed offset. The shift is detected when a point in the sinogram has a speed value deviating by at least 3 m/s from two neighboring points. Figure 13 shows two example situations of detecting a speed shift.

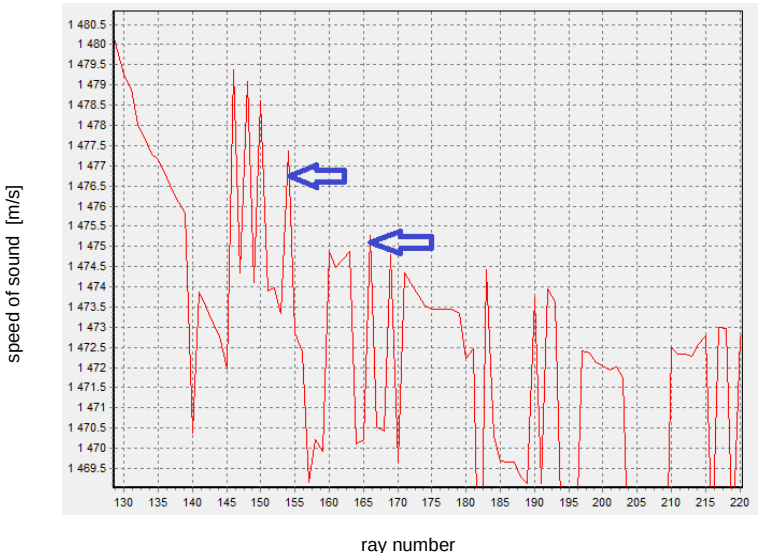

Fig. 13. Example of detecting singly occurring speed shift (marked with arrows)
Rys. 13. Przykład wykrycia pojedynczo występujących przeskoków prędkości

Figure 14 shows a sinogram speed after one cycle of correction of single shifts. One cycle means looking through the sinogram once along the *x* axis and along the *y* axis. As you can see, most of the points of different speed have disappeared from the sinogram. The range of calculated speeds was further reduced to 1463 - 1518 m/s.

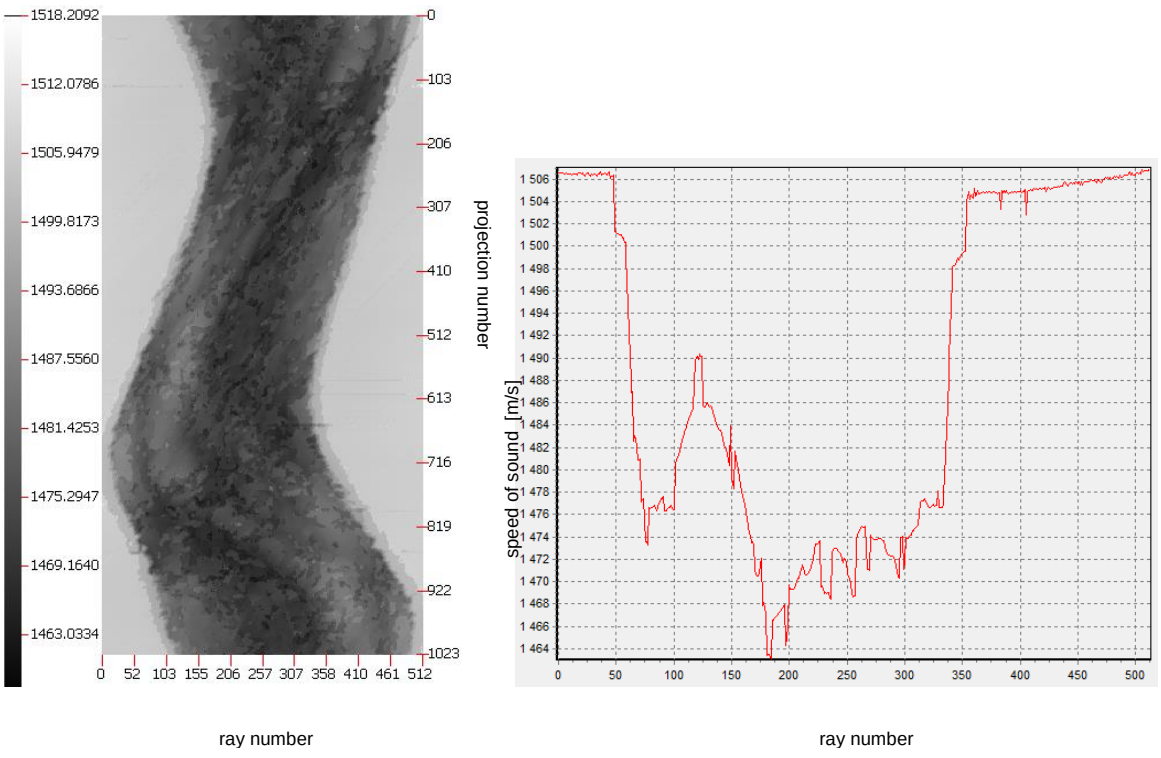

Fig. 14. Sinogram showing the speed of sound values after correction of single shifts (1 correction cycle) and an example of a sinogram line
Rys. 14. Sinogram prędkości po korekcji pojedynczych przeskoków (1 cykl korekcji) i przykładowa linia sinogramu

Figure 15 presents reconstructed images of the breast cross-section from the corrected sinogram.

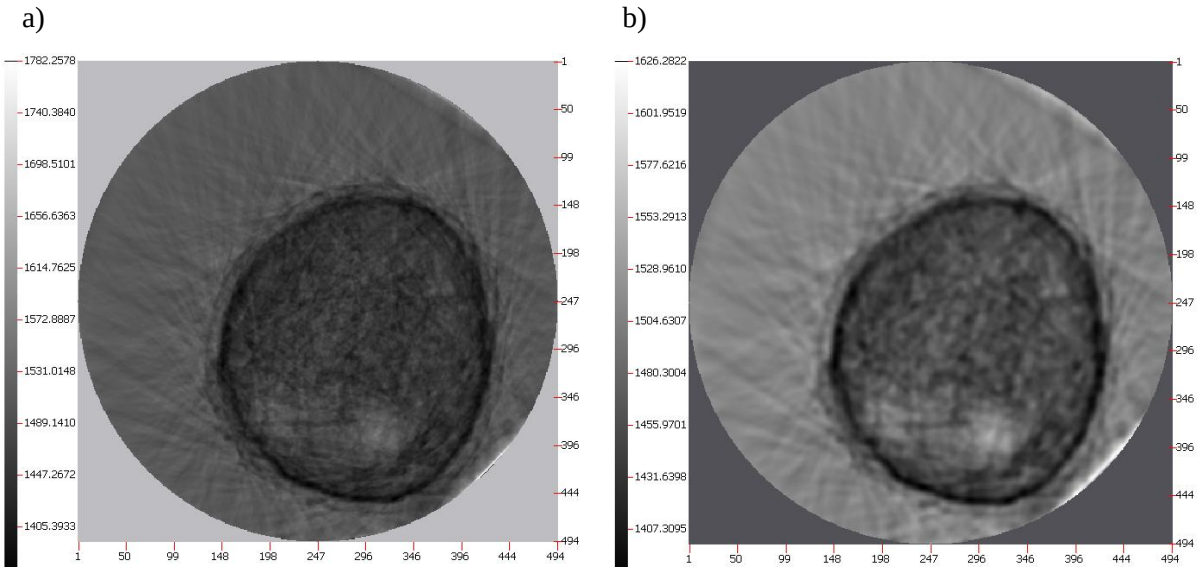

Fig. 15. Reconstructed speed distribution in the cross section of the breast after correction of single shifts (1 correction cycle): with Hamming filter a) with stochastic filter b)

Rys. 15. Zrekonstruowany rozkład prędkości w przekroju piersi po korekcji pojedynczych przeskoków (1 cykl korekcji): z filtracją Hamminga a) z filtrem stochastycznym b)

One cycle of looking through the sinogram does not eliminate all single shifts. Due to the disturbance structure, the "cleaning" operation must be carried out several times. Thus, 10 look through cycles of the sinogram were carried out in succession. Figure 16 shows the sinogram after 10 iterations of the debugging routine. Compared to the previous sinograms (Figs. 8, 10, 14), there are more homogeneous areas with little change in speed value.

The reconstruction of the breast cross-section from the sinogram after 10 iterations of single shift correction is shown in Fig. 17. The image of the breast cross-section reconstructed using Hamming filtering shows a much smaller amount of noise in the form of lines.

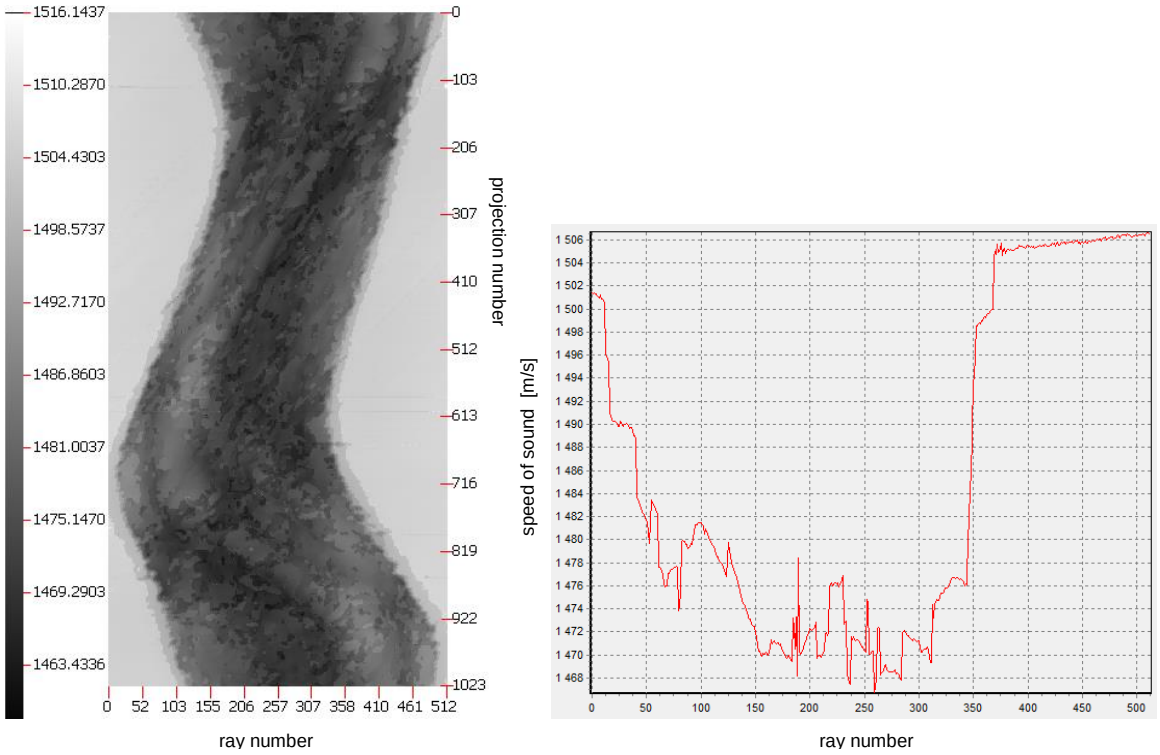

Fig. 16. Sinogram showing the speed of sound values after correction of single shifts (10 correction cycles) and an example of a sinogram line

Rys. 16. Sinogram prędkości po korekcji pojedynczych przeskoków (10 cykli korekcji) i przykładowa linia sinogramu

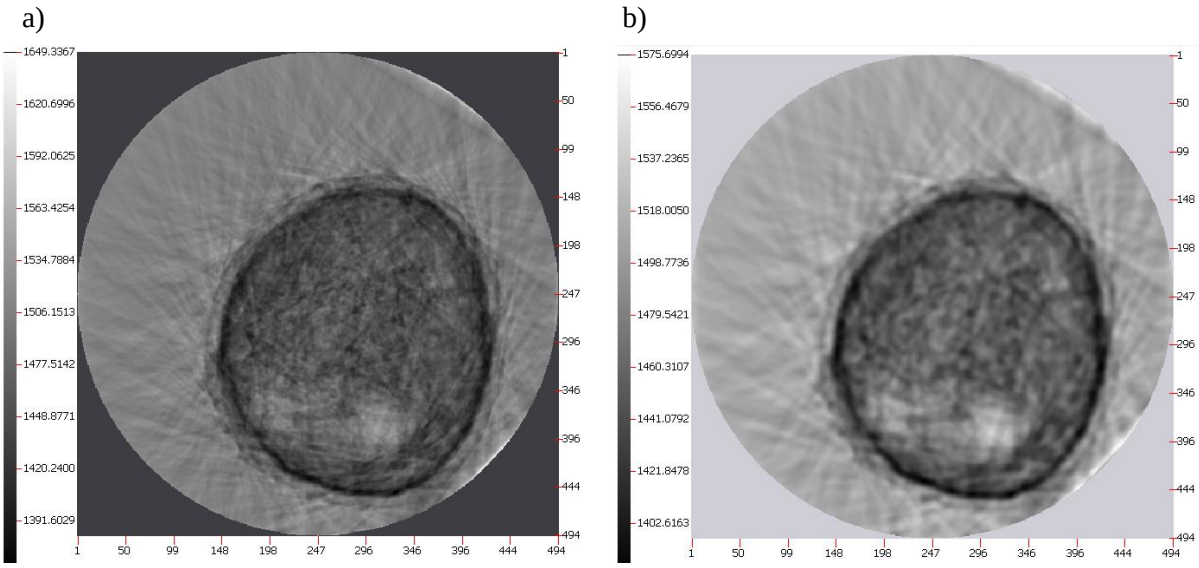

Fig. 17. Reconstructed speed distribution in the cross section of the breast after correction of single shifts (10 correction cycles): with Hamming filter a) with stochastic filter b)

Rys. 17. Zrekonstruowany rozkład prędkości w przekroju piersi po korekcji pojedynczych przeskoków (10 cykli korekcji): z filtracją Hamminga a) z filtrem stochastycznym b)

13.6. Conclusions

The results of the conducted experiments have shown that the determination of the time of passage of the ultrasound wave through the breast tissue with the use of the zero-crossing detection method causes specific disturbances of the reconstructed image. These disturbances result from sudden changes of the determined speed caused by the shift of the detection point by integer multiples of the period of the received pulse. The removal of these disturbances is not trivial as they are mainly related to the phenomenon of multipath during the propagation of the ultrasound wave in the breast tissue.

The experiments have shown that the removal of the presented detection errors gives a significant improvement in the quality of the reconstructed image (compare Fig. 9 vs. 17).

The presented procedure algorithm was used to improve the quality of the obtained images in the prototype ultrasound tomograph.

Bibliography

1. Duric N., Littrup P., Babkin A., Kalinin A., Pevzner R. Tokarev M., Holsapple E., Rama O., Duncan R.: Development of ultrasound tomography for breast imaging: Technical assessment. Medical Physics, 2005, 32(5), 1375-1386.
2. Duric N., Littrup P., Li C., Rama O., Bey-Knight L., Schmidt S., Lupinacci J.: Detection and characterization of breast masses with ultrasound tomography: Clinical results. Proc. of SPIE, 2009, 7265.
3. Duric N., Littrup P., Poulo L., et al.: Detection of breast cancer with ultrasound tomography: First results with the Computed Ultrasound Risk Evaluation (CURE) prototype. Med. Phys. 2007, 34(2), 773-785.
4. Herman G.T.: Fundamentals of computerized tomography: Image reconstruction from projection, 2nd edition. Springer, 2009.
5. Hortobagyi G.N., de la Salazar J.G., Pritchard K., et al.: The global breast cancer burden: variations in epidemiology and survival. Clin. Breast Cancer, vol. 6. 2005, 391-401.
6. Jain A.K.: Fundamentals of Digital Image Processing. Prentice Hall, 1989, USA.
7. Jirik R., Peterlík I., Ruiter N., et al.: Sound-speed image reconstruction in sparse-aperture 3-D ultrasound transmission tomography. IEEE T. Ultrason. Ferr. 59(2), 2012, 254-264.
8. Kak A.C., Slaney M.: Principles of Computerized Tomographic Imaging. IEEE Press, New York 1988.
9. Marmarelis V.Z., Jeong J. et al.: High-resolution 3-D imaging and tissue differentiation with transmission tomography. Acoust. Imag. 28, 2007, 195-206.
10. Opieliński K.J., Gudra T.: Multi-parameter ultrasound transmission tomography of biological media. Ultrasonics, 44, 1–4, 2006, e295-e302.

11. Opieliński K.J., Pruchnicki P., Gudra T., Majewski J.: Conclusions from a test of multi-modal ultrasound tomography research system designed for breast imaging. Proceedings of 7th Forum Acusticum 2014, European Acoustics Association, Kraków 2014.
12. Opieliński K.J., Pruchnicki P., Gudra T., et al.: Ultrasound transmission tomography imaging of structure of breast elastography phantom compared to US, CT and MRI. Arch. Acoust. 38(3), 2013, p. 321-334.
13. Opieliński K.J., Pruchnicki P., Gudra T., et al.: Imaging results of multi-modal ultrasound computerized tomography system designed for breast diagnosis. Comput. Med. Imag. Graph, 2015, 46, 83-94.
14. Opieliński K.J., Pruchnicki P., Gudra T., Podgórski P., Kraśnicki T., Kurcz J., Sąsiadek M.: Breast Phantom Imaging Results from an Ultrasound Computer Tomography Research System. [in:] Information Technologies in Biomedicine (Advances in Intelligent Systems and Computing vol. 283) vol. 3. 2014, 49-60.
15. Opieliński K.J., Pruchnicki P., Jóźwik M., et al.: Breast ultrasound Tomography: preliminary in vivo results. [in:] Piętka E., Badura P., Kawa J., Więcławek W., (eds.): Information Technologies in Medicine (Advances in Intelligent Systems and Computing vol. 471). Springer International Publishing, 2016, 193-205.
16. Quan Y., Huang L.: Sound-speed tomography using first-arrival transmission ultrasound for a ring array. Proceedings of SPIE, 2007, 6513, 651306-1-9.
17. Wiskin, J., Borup, D., Johnson, S., et al.: Three-dimensional nonlinear inverse scattering: Quantitative transmission algorithms, refraction corrected reflection, scanner design and clinical results. POMA, 2013, vol. 19, (075001)

Acknowledgment

The research was performed as project POIR.01.01.01-00-1595/15, titled: “Development of a prototype of multimodal ultrasound tomography system for breast diagnosis” co-financed by European Union from the European Regional Development Fund.